

Simulations of a New Double U-tube Borehole Configuration with Solar Heat Injection and Ground Freezing

Parham Eslami Nejad¹ and Michel Bernier²

¹ Canmet Energy Technology Center, Varennes, Québec

² Département de génie mécanique, École Polytechnique, Montréal, Québec

Abstract

Ground coupled heat pump (GCHP) systems are popular systems for space conditioning and hot water production. However, due to the high drilling costs of the ground loop portion, the initial investment is relatively high. In an attempt to reduce costs, a new borehole configuration has been recently proposed. It consists of a double U-tube borehole with two independent circuits and a saturated sand ring. One circuit is linked to a heat pump to extract heat from the ground and the other is connected to thermal solar collectors for solar heat injection. In effect, the borehole acts as a heat exchanger between the solar collectors and the heat pump.

During peak building loads, usually at night when solar energy is unavailable, the heat pump extracts energy from the ground and in some cases the saturated sand freezes. This slows down the decrease in the return temperature to the heat pump and takes advantage of the relatively high energy content associated with the latent heat of fusion of water in the sand. When solar energy is available, solar heat is injected in the second U-Tube to melt the frozen saturated ring.

The impact of this proposed system on borehole length is dependent on the building loads and the solar heat injection profiles. Preliminary simulation results show that the newly proposed configuration can reduce the borehole length by 18% for a well-insulated building located in Montréal with an annual space heating load of 11850 kWh.

In this study, a parametric analysis is undertaken to study the impact of various building loads and solar energy profiles on borehole length requirements.

1 Introduction

Ground coupled heat pump systems with vertical geothermal boreholes constitute attractive alternatives for space conditioning and domestic hot water production. However, high cost associated with drilling of the boreholes is always a barrier for widespread utilization of these systems particularly in single borehole installations.

During the last decades researchers have proposed different alternatives to reduce the borehole length by using a supplementary source of energy. Most recent studies have combined solar energy and GCHP systems to balance the ground loads and reduce the borehole length. For example, Yang et al. (2010) and Xi et al. (2011) recently indicated that using thermal solar collectors to charge the heat pump evaporator is a feasible way to make GCHP systems attractive for space heating and domestic hot water production in cold climates. Kjellsson et al. (2010) reported that a hybrid system with solar heat injection into the boreholes in winter and solar domestic hot water production during the summer is the option with the highest electrical consumption savings. Chiasson and Yavuzturk (2003) found that solar

heat injection into multiple boreholes can reduce the borehole length and make the system economically viable. However, it has been shown that solar heat injection into a single borehole does not reduce the borehole length significantly (Bernier and Salim Shirazy, 2007). For a fixed borehole length, it was shown that the heat pump energy consumption does not change significantly (Eslami nejad et al., 2009). Furthermore, coupling solar thermal collectors and GCHP systems using typical borehole configuration requires an extra heat exchanger which may add to the complexity (Eslami nejad and Bernier, 2011b) of the system and introduces a source of efficiency loss in the system.

Recently, Eslami nejad and Bernier (2011a, 2011b) developed a new borehole configuration with two fully independent U-tubes. In this configuration, one U-tube is linked to a heat pump and the other is connected to thermal solar collectors and therefore no extra above-ground heat exchanger is needed which translates into reduction of the system complexity. Eslami nejad and Bernier (2011b) performed several simulations for 20 years to examine the impact of thermal recharging of a single-borehole using the proposed configuration. They indicated that despite a relatively large amount of solar energy injected into the system, the annual heat pump energy consumption is not reduced significantly. However, the proposed system might contribute to reduce installation costs as it leads to shorter boreholes. They concluded that since the available solar energy injected into the borehole is not necessarily coincident with the peak building loads it dissipates rapidly into the ground without making proportional effects on borehole depth.

System configuration

The system under study is presented schematically in Figure 1. It consists of a double U-tube borehole with two independent circuits connected to a heat pump and thermal solar collectors. This borehole is surrounded by a relatively small fully saturated (with water) sand ring. During peak building loads, usually at night when solar energy is unavailable, the heat pump extracts energy from the ground and in some cases the saturated sand freezes. This slows down the decrease in the return temperature to the heat pump and takes advantage of the relatively high energy content associated with the latent heat of fusion of water in the sand. When solar energy is available, solar heat is injected in the second U-tube to melt the frozen saturated ring and recharge the borehole for the next heat extraction cycle.

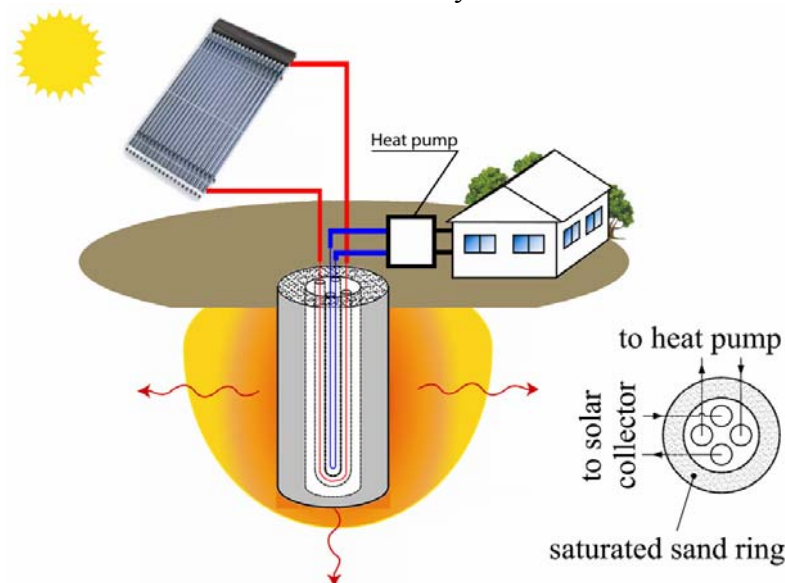


Figure 1: Schematic representation of the system configuration

System simulations of a real heat pump operation are performed with a 6 minute time step to evaluate the merits of the proposed borehole configuration. Furthermore, a parametric

analysis is undertaken to quantify the impact of different building loads and solar energy profiles on borehole length requirements. Three cities in Canada with relatively different climates are considered: Montréal, Edmonton, and Vancouver. The building and solar loads as well as the borehole, ground, heat pump, and solar collector are linked to perform GCHP simulations over one entire heating season.

2 Methodology

In this study, a 1-D numerical heat transfer model of the ground, developed by Eslami nejad and Bernier (2011c), is coupled to an analytical model of a double U-tube borehole with two independent circuits (Eslami nejad and Bernier, 2011b). The ground model accounts for freezing and melting in the immediate vicinity of the borehole (i.e. in the saturated ring) and the borehole model can handle different inlet temperatures as well as different mass flow rates for the two U-tubes. These models are explained briefly in the following subsections; more details are given by Eslami nejad and Bernier (2011c):

Ground model

The ground model is a one-dimensional (1-D) heat conduction model including phase change. The effective heat capacity approach is used to account for freezing and thawing in the saturated ring (Bonacina et al., 1973). Three phases are considered: ice-soil mixture (solid), water-soil mixture (liquid), and a transition phase. Based on procedure outlined by Bonacina et al. (1973) the latent heat effect is approximated by a large effective specific heat over a small temperature range in the transition phase.

Based on these assumptions the governing equation is given by:

$$\rho c \frac{\partial T}{\partial t} = \frac{1}{r} \frac{\partial}{\partial t} \left(kr \frac{\partial T}{\partial r} \right) \quad (1)$$

where ρc is the heat capacity and k is thermal conductivity. These physical properties are constant for a given phase however they can vary from one phase to the other. The calculation domain extends from the borehole wall to the far-field and includes the saturated sand ring. The numerical finite-volume approach of Patankar (1980) is used. According to this technique, Equation (1) is integrated over control volumes using piecewise linear interpolation and over time intervals using the fully-implicit scheme. The resulting coupled set of algebraic equation is solved over the whole domain using a classical tridiagonal matrix algorithm (TDMA).

Borehole model

The numerical ground model described above is coupled to an analytical borehole model of a double U-tube borehole with two independent circuits operating with unequal mass flow rates and inlet temperatures. This model has been described by Eslami nejad and Bernier (2011a, 2011 b). It is a steady-state analytical model which accounts for fluid and pipe thermal resistance and thermal interaction among U-tube circuits and predicts the fluid temperature profiles in both circuits along the borehole depth.

Figure 2 presents a cross-section of a double U-tube borehole where the space between the pipes and the borehole wall is filled with a grout having a thermal conductivity k_b . The pipes, with an external radius r_p , are placed symmetrically in the borehole with identical center-to-center distance ($2D$) between two opposing pipes. In the present work, the 1-3,2-4 configuration is used (Zeng et al., 2003): the fluids from the heat source and the heat pump flow inside circuit 1-3 and 2-4, respectively. In effect, this configuration with two independent circuits acts as a heat exchanger between the heat source and the heat pump. For a given bore-

hole wall temperature, T_b , and inlet conditions from both circuits, the model predicts the outlet temperatures of both circuits.

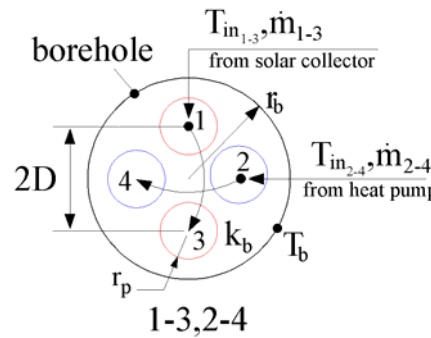


Figure 2: Cross-section of a double U-tube borehole

As shown in Figure 3, the ground and borehole models are coupled at the borehole wall. An iterative solution is used at each time step to link the borehole and ground models: The iteration starts by guessing T_b to calculate the heat transfer rate at the borehole wall, q_b , using the borehole model. Using this result, the ground model then calculates T_b . Calculations continue until the difference between two successive T_b drops below the convergence criteria. A relatively similar two-region model was validated experimentally by Yang et al. (2009). They coupled a steady state single U-tube borehole model to a transient one-dimensional heat conduction ground model based on the cylindrical heat source approach.

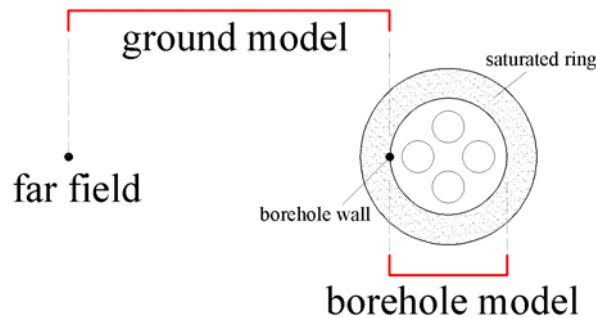


Figure 3: Borehole and ground model calculation domains

3 System simulations

In order to evaluate the merits of the proposed system configuration (presented in Figure 1), two alternatives are compared. The first one, which will be referred to as the reference case (Case 1), is a conventional GCHP system with a regular parallel double U-tube borehole (Figure 4a). Case 2 involves solar recharging using a double U-tube borehole with two independent circuits. In this case, one circuit is linked to the heat pump and the other to thermal solar collectors (Figure 4b). Using this configuration, both circuits can work simultaneously or independently. As shown in Figure 4b, the pipes inside the borehole are in intimate contact and the borehole is surrounded by a saturated sand ring.

Borehole characteristics in Cases 1 and 2 are given in Table 1. Both boreholes have the same overall diameter of 15 cm and are equipped with four 3.34 cm diameter pipes. In Case 2, the sand ring thickness ($r_{sr} - r_b$) is 3.4 cm. Grout thermal conductivity, k_b , is $2 \text{ W}\cdot\text{m}^{-1}\cdot\text{K}^{-1}$ and the saturated sand ring thermal conductivity in Case 2, k_r , is $3 \text{ W}\cdot\text{m}^{-1}\cdot\text{K}^{-1}$. Based on a successful model-experiment comparison, the thermal conductivity of the saturated sand ring was also assumed to be equal to $3 \text{ W}\cdot\text{m}^{-1}\cdot\text{K}^{-1}$.

For Case 1, the borehole model of Zeng et al. (2003) is used while Case 2 uses the double U-tube borehole model with two independent circuits developed by Eslami nejad and Bernier (2011b).

A parametric analysis is performed to quantify the impact of different building loads and solar energy profiles on borehole length requirements. Three Canadian cities are considered: Montréal, Edmonton, and Vancouver. The ground thermal conductivity and diffusivity are set to typical values of $2 \text{ W}\cdot\text{m}^{-1}\cdot\text{K}^{-1}$ and $0.08 \text{ m}^2\cdot\text{day}^{-1}$, respectively for all three locations. However, the undisturbed far-field ground temperatures are set to different values of 10°C , 13°C and 7°C for Montréal, Vancouver and Edmonton, respectively.

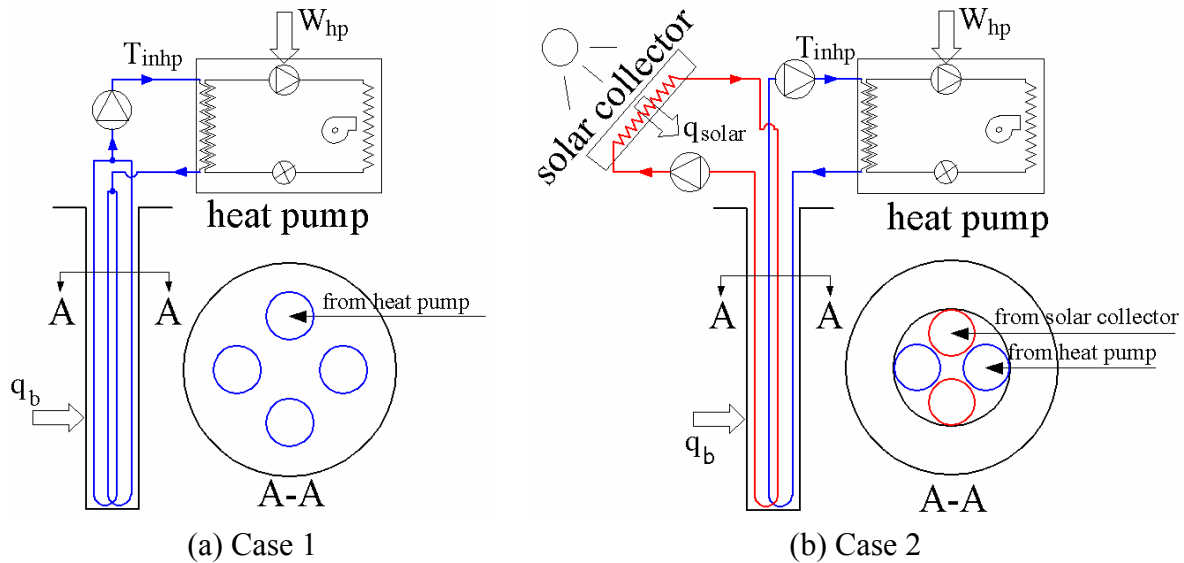


Figure 4: Schematic representation of Cases 1 and 2

Table 1: Borehole characteristics

borehole types	r_b (cm)	r_p (cm)	$2D$ (cm)	r_{sr} (cm)	k_b ($\text{W}\cdot\text{m}^{-1}\cdot\text{K}^{-1}$)	k_r ($\text{W}\cdot\text{m}^{-1}\cdot\text{K}^{-1}$)
Case 1	7.5	1.67	7.5	-	2	-
Case 2	4.1	1.67	4.8	7.5	2	3

Building loads

GCHP system simulations are carried out over an entire heating season using a 6 minute overall time step with the heat pump cycling on and off to meet the building loads. The hourly heating loads of a well-insulated 150 m^2 building are presented in Figure 5 for the three studied cities. These profiles were generated using TRNSYS (Type 56) with a temperature set point in heating mode equal to 20°C .

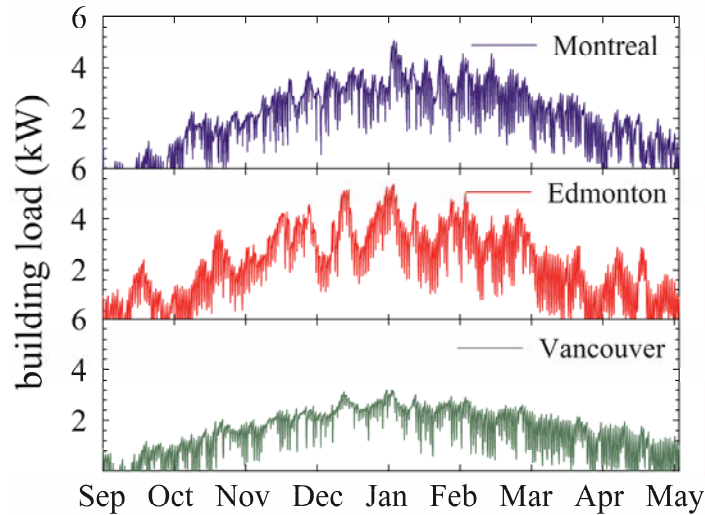


Figure 5: Building heating loads during the heating season in three Canadian cities

As shown in Figure 5, peak space heating loads of 5.0 kW, 5.4 kW and 3.2 kW have been calculated for Montréal, Edmonton and Vancouver, respectively. The annual space heating requirement over the heating season (mid-September to mid-May) is 11850 kWh in Montréal and it is 12740 and 8880 in Edmonton and Vancouver, respectively. It is assumed that during the summer, the building heating load is zero and that the GCHP system does not work.

Heat pump

For all three climates the building is heated with a single-capacity GCHP. The heating capacity and compressor power requirements of the GCHP are given in Figure 6 as a function of the inlet temperature to the heat pump. These characteristics are based on a commercially available 3-ton (10.5 kW) water-to-water GCHP with a mass flow rate on the evaporator side equal to 0.44 kg/s. As shown in Figure 6, the operation of this heat pump is not recommended when the inlet temperature is below -6°C .

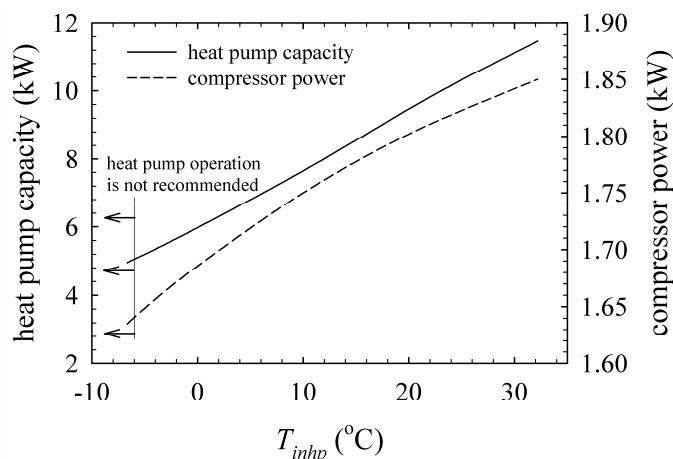


Figure 6: Heat pump capacity and corresponding compressor power requirement as a function of the inlet temperature

Solar collector

The solar collector is a standard single-glazed flat plate collector whose efficiency can be described by a second order curve relating the efficiency to $(T_{mean}-T_a)/G$, Equation (2), where

T_{mean} is the mean fluid temperature in the collector, T_a is the ambient temperature, and G is the incident solar radiation.

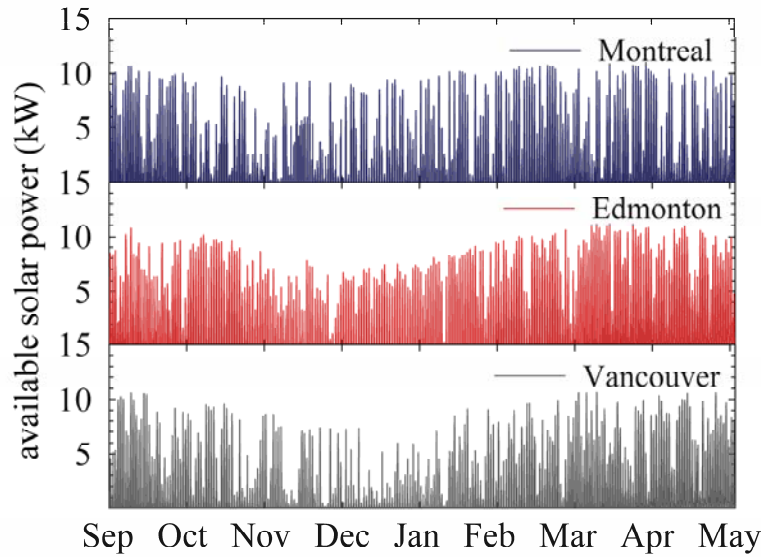


Figure 7: Available solar power during the heating season for three cities in Canada

$$\eta_{collector} = a + b \times \frac{T_{mean} - T_a}{G} + c \times \frac{(T_{mean} - T_a)^2}{G} \quad (2)$$

$$a = 0.78, \quad b = 3.20 \text{ (} W \cdot m^{-2} \cdot K^{-1} \text{)}, \quad c = 0.015 \text{ (} W \cdot m^{-2} \cdot K^{-2} \text{)}$$

The collector area is set at 10 m^2 and the circulating mass flow rate is equal to 0.11 kg/s . Figure 7 presents available solar radiation over the heating season captured by 10 m^2 solar collectors for three cities. The maximum solar radiation is equal to 11, 11.2 and 10.6 kW and the cumulative available solar radiation over the heating season is equal to 9940, 8710, and 7210 kWh for Montréal, Edmonton and Vancouver, respectively.

4 Results and discussion

Results, including required borehole length (H), cumulative heat pump energy consumption (W_{hp}), extracted energy from the ground (q_b), injected solar energy to the borehole (q_{solar}) and annual averages of inlet temperature to the heat pump (T_{inhp}) are presented in Table 2 for Cases 1 and 2 located in Montréal, Edmonton and Vancouver. Figure 8 presents the location of the freezing interface in the saturated ring for all three cities (recall that the saturated sand ring extends from a radius of 4.1 cm up to 7.5 cm). The y-axis represents the number of hours from the start (mid-September) to the end of the heating season (mid-May), i.e. a total of 5800 hours.

The resulting borehole lengths required are 71, 50 and 95 m for Case 1 in Montréal, Vancouver and Edmonton, respectively. The corresponding values for Case 2 are 58, 44 and 83 m . These values are the borehole lengths required to keep T_{inhp} above -6°C at all times during the heating season while satisfying the building loads. Due to the fact that the required borehole length is driven by the peak building load and undisturbed ground temperature, the borehole located in Edmonton is the longest and the one in Vancouver is the shortest as they experience the highest (5.4 kW) and the lowest (3.2 kW) peak building loads as well as the lowest and highest undisturbed ground temperature.

As shown in Table 2, for the reference case (Case 1) in Montréal, the heat pump extracts 8260 kWh from the ground (q_b) and uses 3590 kWh for the compressor (W_{hp}) to provide the required building load of 11850 kWh (q_{build}). However, in Case 2, 5750 kWh of solar heat is

injected into the borehole which reduces the amount of energy extracted from the ground by 67% compared to Case 1 (from 8260 down to 2700 kWh). Furthermore, the required borehole length decreases by 13 m (18%). As shown in Table 2, the annual averages of T_{inhp} are -2.0°C and 1.0°C for Cases 1 and 2, respectively. This leads to a 5.3% decrease in heat pump energy consumption (from 3590 down to 3400 kWh) despite the fact that the borehole is 18% shorter. The higher value of T_{inhp} for Case 2 is due to solar heat injection into the ground and to freezing of the saturated ring which tends to keep the borehole wall temperature closer to the freezing point.

Table 2: Results of annual simulations

Cities	Montréal		Vancouver		Edmonton	
	CASE					
	1	2	1	2	1	2
q_{build} (kWh)	11850	11850	8880	8880	12740	12740
H (m)	71	58	50	44	95	83
W_{hp} (kWh)	3590	3400	2690	2520	3850	3620
q_b (kWh)	8260	2700	6190	1940	8890	2300
q_{solar} (kWh)	0	5750	0	4420	0	6820
T_{inhp} ($^{\circ}\text{C}$)	-2.0	1.0	-2.4	1.6	-2.1	1.5

As shown in Table 2, the amount of solar energy injected into the borehole in Case 2 increases by 1070 kWh (16%) from 5750 kWh in Montréal to 6820 kWh in Edmonton. However the building load increases only by 890 kWh (7%) from 11850 kWh in Montréal to 12740 kWh in Edmonton. In spite of the higher solar to building load ratio (q_{solar}/q_{build}) of Edmonton (0.53 compared to 0.48 for Montréal) the borehole length is reduced by 12 m (only 13%) from Case 1 to Case 2 whereas the borehole length reduction in Montréal is 18% as mentioned earlier. This is due to the fact that the borehole length is mostly driven by the peak load (the undisturbed ground temperature is not as much a factor for the saturated sand ring) and thus availability of solar energy at peak load has a key effect on required borehole length. As shown in Figure 8, the freezing interface reaches the limit of the saturated sand ring at peak conditions for a relatively long period. This seems to indicate that the extra available solar energy (when compared to Montréal) is not necessarily coincident with the peak building load. Thus, at peak building load conditions the borehole wall temperature will drop below 0°C , which implies that the borehole has to be longer to compensate. It is worth mentioning that the borehole length reduction from Case 1 to Case 2 in Vancouver is 6 m (12%) while it is expected to be more than for Montréal since the solar to building load ratio (q_{solar}/q_{build}) is higher in Vancouver (0.50). As shown in Figure 8, the saturated sand ring seldom freezes in Vancouver. Thus, solar energy is less useful in melting the ring than in Montréal and it is free to diffuse to the soil. As shown in Table 2 for both Cases 1 and 2, the heat pump located in Vancouver consumes less energy compared to the heat pumps in Edmonton and Montréal due to the higher ground temperature and less building load requirements. Furthermore, from Case 1 to Case 2 the heat pump energy consumption in Vancouver decreases by 6.3% (from 2690 to 2520 kWh) since the annual averages of T_{inhp} increases from -2.4°C to 1.6°C . About the same reduction in heat pump energy consumption (by 6.0% from 3850 to 3620 kWh) can be observed for Edmonton which is correspondingly due to the increase in annual averages of T_{inhp} from -2.1°C to 1.5°C .

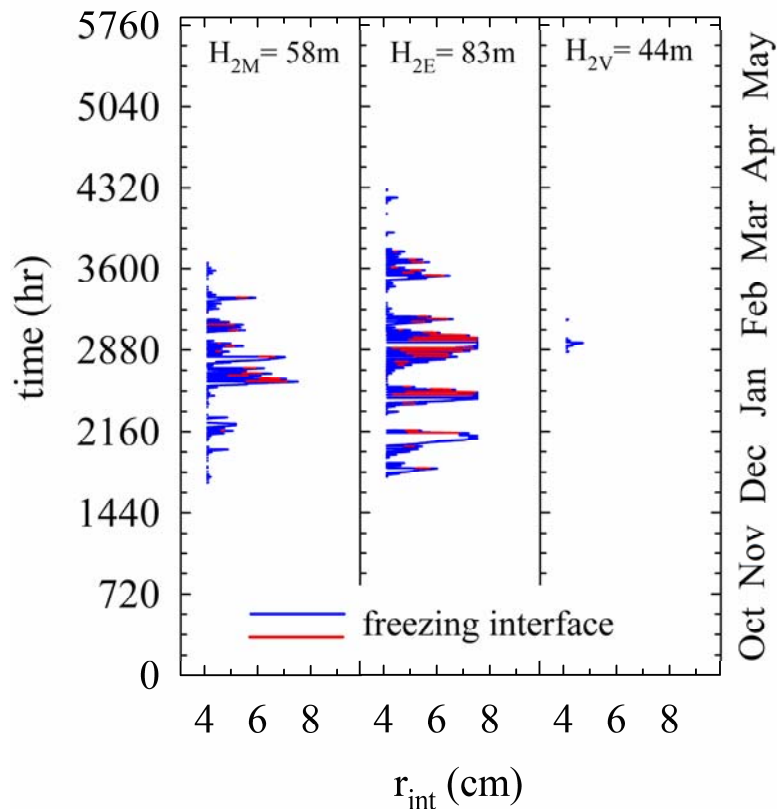


Figure 8: Freezing interface, r_{int} , for Cases 2 (from left to right: Montréal, Edmonton and Vancouver)

It is interesting to now look at the results of Figure 8. For Montréal, freezing of the saturated sand ring starts after 1700 hours of operation. This slows down the decrease in the return temperature to the heat pump (T_{inhp}) and takes advantage of the relatively high energy content associated with the latent heat of fusion of water in the sand. When solar energy is available, it is injected to the borehole to melt the frozen region and recharge the borehole for the next heat pump operation cycle. Consequently, except for short periods, for example at about $t=2600$ hours when the building load is maximum, the saturated sand ring does not freeze entirely and the borehole wall temperature does not fall below the freezing temperature. When the solar availability is high, the frozen ring starts melting rapidly and the borehole wall temperature increases significantly which leads to an increase in T_{inhp} . When solar injection is present there are cases when there are two freezing interfaces. The radiuses of these two interfaces are indicated in blue and red in Figure 8. Finally, when the building load is relatively small, at the beginning and at the end of the simulation period, the saturated ring is unfrozen indicating that the injected solar energy and the net heat flow from the far-field to the borehole is sufficient for heat pump operation.

The figure at the center shows the evolution of the freezing interface for Edmonton. The saturated ring starts freezing at about the same time as in Montréal. However, during some periods most importantly around $t=2100$, 2470 and 2900 hours, the whole saturated ring freezes and it remains frozen for a few hours. For example for the period when the building load is maximum (for $t=2900$ hours) the ring remains frozen for more than 36 hours. During this period solar energy is not available to melt the frozen region. Due to this behavior, the proposed borehole configuration in Edmonton does not contribute to the borehole length reduction as much as this configuration does in Montréal. A bigger saturated ring around the borehole in Edmonton could potentially reduce the borehole length required even more.

Finally, the figure on the right presents r_{int} for the borehole located in Vancouver. As shown in this figure, the saturated ring freezes during a relatively small period. Furthermore, the saturated ring does not freeze completely during the simulation period even during the peak building load. This is due to the fact that the borehole length is too short (44m) to keep the outlet temperature to the heat pump above -6°C with borehole wall temperature of 0°C (during freezing) and to a higher undisturbed ground temperature

5 Conclusion and recommendations

In this study, a parametric analysis is performed to evaluate the impact of various building loads and solar energy profiles on the borehole length requirements of a newly proposed borehole configuration.

This borehole consists of a double U-tube borehole with two independent circuits and a saturated sand ring. One circuit is linked to a heat pump to extract heat from the ground and the other is connected to thermal solar collectors for solar heat injection. During peak heat load conditions, the saturated sand ring is allowed to freeze to take advantage of the large constant-temperature storage capacity offered by the latent heat of fusion of the water. Using this borehole configuration solar energy can be injected, when available, to melt the saturated ring.

Typical borehole configurations are compared against this newly proposed borehole to examine the merits of this configuration. Typically, freezing occurs within a thickness of 3-4 centimetres around the borehole. When solar energy is available and it is injected into one circuit of the borehole, it is shown that it is possible to melt the ice and "recharge" the saturated sand region for the next freezing cycle. With this approach, the borehole length can be reduced by as much as 18% in Montréal. It is worth noting that despite this reduced length, the heat pump energy consumption is reduced as well by 5.3%.

Three cities in Canada with relatively different climates are considered, Montréal, Edmonton, and Vancouver. Six different simulations over an entire heating season are undertaken. Results indicated that using the newly proposed borehole configuration can reduce the borehole length by 18%, 13% and 12% in Montréal, Edmonton and Vancouver, respectively. In spite of shorter boreholes, the proposed borehole configuration reduces the heat pump energy consumption by 5.3%, 6.0% and 6.3% in Montréal, Edmonton and Vancouver, respectively. This is essentially due to the fact that the annual average return temperature to the heat pump is higher with a saturated sand ring.

The numerical ground model used in the present work is based on a number of simplifying assumptions including 1-D radial heat transfer. This is a good engineering approximation to establish that freezing of a saturated ring has some potential while limiting simulation time over a heating season to reasonable values. However, it is clear that a multi-dimensional model that accounts for moisture migration is the next logical step.

6 Acknowledgements

The financial support provided by CanmetENERGY-Varennes and the NSERC Smart Net-zero Energy Buildings Strategic Network is greatly acknowledged.

7 Nomenclature

1-D	One-dimensional
$2D$	Shank spacing between the U-tubes (m)
G	Solar radiation ($\text{W}\cdot\text{m}^{-2}$)
GCHP	Ground coupled heat pump

k_b	Grout thermal conductivity ($\text{W}\cdot\text{m}^{-1}\cdot\text{K}^{-1}$)
k_g	Ground thermal conductivity ($\text{W}\cdot\text{m}^{-1}\cdot\text{K}^{-1}$)
k_r	Saturated sand ring thermal conductivity ($\text{W}\cdot\text{m}^{-1}\cdot\text{K}^{-1}$)
\dot{m}	Mass flow rate of the circulating fluid ($\text{kg}\cdot\text{s}^{-1}$)
q_b	Extracted energy from the ground (kWh)
q_{build}	building load (kWh)
q_{solar}	Solar energy injected into the borehole (kWh)
r_{int}	Freezing interface radius in the saturated region (m)
r_p	Pipe external radius (m)
r_{sr}	Saturated sand ring radius (m)
T_a	Ambient temperature ($^{\circ}\text{C}$)
T_b	Borehole wall temperature ($^{\circ}\text{C}$)
T_{inhp}	Inlet fluid temperature to the heat pump ($^{\circ}\text{C}$)
T_{mean}	Solar collector mean fluid temperature ($^{\circ}\text{C}$)
W_{hp}	Annual heat pump energy consumption (kWh)
$\eta_{\text{collector}}$	Thermal solar collector efficiency
ρc	Heat capacity ($\text{J}\cdot\text{m}^{-3}$)

Subscripts

1-3	1-3 circuit in the 1-3,2-4 configuration
2-4	2-4 circuit in the 1-3,2-4 configuration

8 References

- Bernier, M. & Salim Shirazi, A., 2007. *Solar heat injection into boreholes: a preliminary analysis*, Proceeding of 2nd Canadian Solar Building Conference: T1-1-1, 8 pages.
- Bonacina, C., Comini, G., Fasano, A. & Primicerio, M., 1973. *Numerical solution of phase-change problems*, International Journal of Heat and Mass Transfer: 16(10), 1825-1832.
- Chiasson, A. D. & Yavuzturk, C., 2003. *Assessment of the viability of hybrid geothermal heat pump systems with solar thermal collectors*, ASHRAE Transactions: 109 (2), 487-500.
- Eslami nejad, P. & Bernier, M., 2011a. *Heat transfer in double U-tube boreholes with two independent circuits*, ASME Journal of Heat Transfer: 133(8).
- Eslami nejad, P. & Bernier, M., 2011b. *Coupling of geothermal heat pumps with thermal solar collectors using double U-tube borehole with two independent circuits*, Applied Thermal Engineering: 31(14-15), 3066-3077.
- Eslami nejad, P. & Bernier, M., 2011c. *Freezing of geothermal borehole surroundings: A numerical and experimental assessment with application*, Applied Energy: submitted (October 2011)
- Eslami nejad, P., Langlois, A., Chapuis, S., Bernier, M. & Faraj, W., 2009. *Solar heat injection into boreholes*, Proceeding of 4th Canadian Solar Building Conference: 237-246.

- Kjellsson, E., Hellström, G. & Perers, B., 2010. *Optimization of systems with the combination of ground-source heat pump and solar collectors in dwellings*, *Energy*: 35 (6), 2667-2673.
- Patankar, S. V., 1980. *Numerical heat transfer and fluid flow* 2nd ed., New York: McGraw-Hill.
- Xi, C., Lin, L. & Hongxing, Y., 2011. *Long term operation of a solar-assisted ground coupled heat pump system for space heating and domestic hot water*, *Energy and Buildings*: 43(8), 1835-1844.
- Yang, H., Cui, P. & Fang, Z., 2010. *Vertical- borehole ground-coupled heat pumps: A review of models and systems*, *Applied Energy*: 87 (1), 16-27.
- Yang, W., Shi, M., Liu, G. & Chen, Z., 2009. *A two-region simulation model of vertical U-tube ground heat exchanger and its experimental verification*, *Applied Energy*: 86 (10), 2005-2012.
- Zeng, H., Diao, N. & Fang, Z., 2003. *Heat transfer analysis of boreholes in vertical ground heat exchangers*, *International Journal of Heat and Mass Transfer*: 46 (23), 4467-4481.